Chinese Journal of Natural Medicines

Gambogenic acid induces apoptosis *via* upregulation of Noxa in oral squamous cell carcinoma

Xinran CHENG, Mengyuan FENG, Anjie ZHANG, Jian GUO, Yunlai GONG, Xiaohui HU, Quanbin HAN, Shengbao LI, Xianjun YU

Citation: Xinran CHENG, Mengyuan FENG, Anjie ZHANG, Jian GUO, Yunlai GONG, Xiaohui HU, Quanbin HAN, Shengbao LI, Xianjun YU, Gambogenic acid induces apoptosis *via* upregulation of Noxa in oral squamous cell carcinoma, Chinese Journal of Natural Medicines, 2024, 22(7), 632−642. doi: 10.1016/S1875−5364(24)60578−9.

View online: https://doi.org/10.1016/S1875−5364(24)60578−9

Available online at www.sciencedirect.com
ScienceDirect
Chinese Journal of Natural Medicines 2024, **22**(7): 632-642
doi: 10.1016/S1875-5364(24)60578-9
Chinese Journal of Natural Medicines

•Original article•

Gambogenic acid induces apoptosis *via* upregulation of Noxa in oral squamous cell carcinoma

CHENG Xinran[1, 2, 3Δ], FENG Mengyuan[2, 3Δ], ZHANG Anjie[2, 3Δ], GUO Jian[1, 2], GONG Yunlai[2, 3], HU Xiaohui[2, 3], HAN Quanbin[3, 4], LI Shengbao[1, 3*], YU Xianjun[1, 2, 3*]

[1] *Department of Gastroenterology, Taihe Hospital, Hubei University of Medicine, Shiyan 442000, China;*
[2] *Laboratory of Inflammation and Molecular Pharmacology, School of Basic Medical Sciences & Biomedical Research Institute, Hubei Key Laboratory of Wudang Local Chinese Medicine Research, School of Pharmacy, Hubei University of Medicine, Shiyan 442000, China;*
[3] *Inflammation-Cancer Transformation and Wudang Chinese Medicine Research, Hubei Talent Introduction and Innovation Demonstration Base, Hubei University of Medicine, Shiyan 442000, China;*
[4] *School of Chinese Medicine, Hong Kong Baptist University, Hong Kong 999077, China*

Available online 20 Jul., 2024

[ABSTRACT] Gambogenic acid (GNA), a bioactive compound derived from the resin of *Garcinia hanburyi*, has demonstrated significant antitumor properties. However, its mechanisms of action in oral squamous cell carcinoma (OSCC) remain largely unclear. This study aimed to elucidate the apoptotic effects of GNA on OSCC cell lines CAL-27 and SCC-15. Our results indicated that GNA induced apoptosis by upregulating the pro-apoptotic protein Noxa. Mechanistic investigations revealed that GNA treatment led to the generation of reactive oxygen species (ROS), which activated endoplasmic reticulum (ER) stress, culminating in cell apoptosis. Inhibition of ROS production and ER stress pathways significantly mitigated GNA-induced Noxa upregulation and subsequent apoptosis. Furthermore, *in vivo* studies using a murine xenograft model demonstrated that GNA administration effectively inhibited the growth of CAL-27 tumors. Collectively, these findings underscore GNA's potential as a therapeutic agent for the treatment of OSCC.

[KEY WORDS] Oral squamous cell carcinoma; Gambogenic acid; Apoptosis; Noxa; ROS/ER stress
[CLC Number] R965 **[Document code]** A **[Article ID]** 2095-6975(2024)07-0632-11

Introduction

Oral squamous cell carcinoma (OSCC), a prevalent malignancy of the head and neck, ranks as the fourth leading cause of cancer-related mortality in Asia [1]. Although advancements in surgery, radiotherapy, and chemotherapy have improved OSCC outcomes, these treatments are often limited by significant side effects and the development of drug resistance, resulting in poor patient survival rates [2]. Therefore, there is a critical need for novel therapeutic strategies and more effective anticancer agents to enhance OSCC treatment and prevention.

Noxa, a pro-apoptotic protein characterized by a Bcl-2 homology 3 domain, is activated by various stimuli. During apoptosis, Noxa translocates to the mitochondrial membrane, prompting cytochrome C release, caspase activation, and eventual cell death [3]. Inhibition of Noxa through knockdown or knockout significantly reduces apoptosis in tumor cells exposed to stimuli such as irradiation, DNA damage, excessive reactive oxygen species (ROS), and endoplasmic reticulum (ER) stress [3, 4]. Thus, Noxa is a promising intracellular target for cancer therapy.

Natural compounds and their derivatives are rich sources of anticancer drugs. Gambogenic acid (GNA), extracted from the traditional Chinese medicine Gamboge, is known for its

[Received on] 18-Jan.-2024
[Research funding] This work was supported by the Projects of International Cooperation and Exchanges (No. G2022027012L), the Natural Science Foundation of Hubei Provincial Department of Education (No. T2022021), the Advantages Discipline Group (Medicine) Project in Higher Education of Hubei Province (2021-2025) (Nos. 2024XKQY26 and 2023BMXKQY2), the Open Project of Hubei Key Laboratory of Wudang Local Chinese Medicine Research of Hubei University of Medicine (No. WDCM2023007), the Innovative Research Program for Graduates of Hubei University of Medicine (No. YC2022033,YC2024003).
[*]**Corresponding author]** E-mails: libao@taihehospital.com (LI Shengbao); xjyu@hbmu.edu.cn (Yu Xianjun)
[Δ]These authors contributed equally to this work.
These authors have no conflict of interest to declare.

antioxidant, anti-inflammatory, and anti-infective properties [5]. Recent research has highlighted GNA's potent antitumor effects [6-9]. However, the specific effects and molecular mechanisms of GNA in human OSCC cells remain insufficiently explored.

Our study demonstrated that GNA induced apoptosis in OSCC cells through a Noxa-dependent mechanism. We found that GNA upregulated Noxa, leading to apoptosis *via* the induction of excessive ROS and ER stress. These findings suggested that GNA has significant potential as an effective therapeutic agent for the treatment of OSCC.

Material and Methods

Reagents

GNA was obtained from Shanghai Yuanye Bio-Technology Company (Shanghai, China). *N*-acetyl-L-cysteine (NAC), 4-phenylbutyrate (4-PBA), SP600125, Z-VAD-FMK, and dimethyl sulfoxide (DMSO) were purchased from MCE (Shanghai, China). Primary antibodies against poly ADP-ribose polymerase (PARP), cleaved caspase-3, Noxa, tumor necrosis factor receptor-associated factor 2 (TRAF2), phospho-JNK (Thr183/Tyr185), JNK, phospho-inositol-requiring transmembrane kinase/endoribonuclease 1α (p-IRE1α, Ser-724), IRE1α, phospho-apoptosis signal-regulating kinase 1 (p-ASK1, Thr845), and ASK1 were purchased from Cell Signaling Technology (CST, Danvers, MA, USA). Glucose-regulated protein 78 (GRP78), activating transcription factor 6 (ATF6), and C/-EBP homologous protein (CHOP) were purchased from Santa Cruz Biotechnology (NY, USA). GAPDH was purchased from Wuhan Servicebio Technology (Wuhan, China). The secondary antibodies were obtained from Jackson Labs (West Grove, PA, USA). Fetal bovine serum (FBS) was purchased from QmSuero/Tsingmu Biotechnology (Wuhan, China).

Cell culture

Human OSCC cell lines CAL-27 and SCC-15 were cultured in Dulbecco's Modified Eagle Medium (DMEM; Thermo Fisher Scientific, Inc., Waltham, MA, USA) supplemented with 10% FBS and penicillin/streptomycin (Thermo Fisher Scientific, Inc., Waltham, MA, USA). The cells were maintained in a humidified incubator at 37 °C with 5% CO_2.

Cell proliferation assay

CAL-27 and SCC-15 cells were seeded at a density of 5×10^3 cells per well in 96-well plates. The cells were then treated with various concentrations of GNA for 24 or 48 h. Following treatment, 10 μL of MTT solution (Beyotime, Shanghai, China) was added to each well and incubated for 4 h. Absorbance was measured at a wavelength of 490 nm using a microplate reader (Bio-Tek Instruments).

Colony formation assay

CAL-27 and SCC-15 cells were seeded at a density of 500 cells per well in 12-well plates. The cells were treated with various concentrations of GNA, with the medium being replaced with fresh medium every 3 days. After two weeks, the colonies were washed, fixed with 4% paraformaldehyde, and stained with 0.1% crystal violet to facilitate colony counting.

Flow cytometric analysis of apoptosis

The proportion of apoptotic cells was determined using an Annexin V/PI Apoptosis Detection Kit (#BB-4101, BestBio, Shanghai, China) according to the manufacturer's instructions. Cells were treated with GNA and other interventions for the specified durations, then harvested and resuspended in the appropriate buffer. Five microliters of Annexin V were added to the cell suspension, and the mixture was incubated in the dark for 30 min. Subsequently, 10 μL of PI solution was added, and the proportion of apoptotic cells was analyzed using a flow cytometer (Beckman Coulter, USA).

Measure of ROS

ROS levels were assessed using a ROS assay kit (Beyotime, China). Briefly, 2×10^5 cells were treated with GNA and other interventions for 12 h. Following treatment, the cells were incubated with 7-dichlorofluorescin-diacetate (DCFH-DA) for 30 min at 37 °C. The cells were then washed with serum-free DMEM to remove any nonspecific binding. ROS levels were measured using fluorescence microscopy (Olympus, Japan).

Detection of gene expression

Total RNA was extracted from cells using TRIzol reagent (Vazyme Biotech Co., Ltd., Nanjing, China) according to the manufacturer's protocol. Cold chloroform was added to the lysed cells, followed by a 30-min incubation. The supernatants were collected and incubated with isopropanol to precipitate the RNA. Reverse transcription was performed using the reverse transcription polymerase chain reaction (RT-PCR) kit (Vazyme Biotech Co., Ltd., Nanjing, China) to synthesize cDNA. The mRNA levels of target genes were quantified using SYBR Premix Ex Taq (TaKaRa, Dalian, China), and relative expression levels were calculated using the comparative C_t method.

Western blotting and immunoprecipitation assays

Cells and tissues were lysed using RIPA buffer supplemented with a protease inhibitor (MCE, Shanghai, China). Protein concentrations were quantified, and equal amounts of protein were separated by SDS-polyacrylamide gel electrophoresis. The proteins were then transferred to polyvinylidene difluoride (PVDF) membranes. The membranes were blocked with 5% nonfat milk for 1 h and subsequently incubated with primary antibodies overnight at 4 °C. The following day, the membranes were incubated with secondary antibodies and visualized using a ChemiDoc Imaging System (Bio-Rad, CA, USA). For immunoprecipitation analysis, cell lysates were incubated with primary antibodies overnight at 4 °C with gentle rocking. The next day, the lysates were mixed with Protein G Agarose beads (Invitrogen, USA) and incubated for an additional 2 h at 4 °C. The beads were washed with ice-cold lysis buffer and boiled for 7 min. The resulting immunoprecipitates were subjected to Western blotting analysis.

CAL-27 xenograft model

The animal experiment was conducted at the Experimental Animal Center of Hubei University of Medicine, China, and approved by the Ethics Committee of Hubei University of Medicine (approval number: 2020-053). Nude mice (BALB/c-nu/nu) were purchased from Weitong Lihua Experimental Animal Technical Company (Beijing, China). CAL-27 cells (1×10^6 cells) were subcutaneously injected into the flanks of the mice. When tumor volume reached approximately 100 mm^3, the mice were randomized into four groups: vehicle control, GNA treatment groups (1 and 2 $mg \cdot kg^{-1}$), and a positive control group receiving paclitaxel (PTX). Tumor size was measured, and volume was calculated using the formula: length × $width^2$ × 0.5. Eighteen days after injection, the mice were euthanized using isoflurane, and serum and tumor tissues were collected for subsequent analysis.

Statistical analysis

Experimental data were analyzed using GraphPad Prism software. Results are presented as mean ± SD. Statistical significance was determined with $^*P < 0.05$.

Results

GNA suppresses cell proliferation and triggers apoptosis in human OSCC cells

To evaluate the effect of GNA (Fig. 1A) on cell proliferation, OSCC cell lines CAL-27 and SCC-15 were treated with GNA for 24 or 48 h, and cell proliferation was assessed using MTT assays. The results indicated that GNA significantly inhibited the proliferation of CAL-27 and SCC-15 cells in a concentration- and time-dependent manner (Fig. 1B). To further assess the impact of GNA on cell viability, trypan blue staining was performed, which revealed a marked reduction in cell viability following GNA treatment (Fig. 1C). Additionally, colony formation assays demonstrated that GNA significantly suppressed colony formation in both cell lines (Fig. 1D).

To explore the relationship between cell growth inhibition and apoptosis, we investigated the effect of GNA on apoptosis. CAL-27 and SCC-15 cells were treated with GNA, and the levels of apoptotic marker proteins were examined. Compared to untreated cells, GNA significantly increased the levels of cleaved PARP and caspase-3 in a concentration- and time-dependent manner, while the expression of PCNA decreased with GNA treatment (Figs. 1E and 1F, Supplementary Figs. S1A and S1B). Further analysis of GNA-induced apoptosis in CAL-27 and SCC-15 cells was conducted using Annexin V-PI double staining and flow cytometry. The proportion of Annexin V/PI double-stained cells was significantly elevated following GNA treatment (Fig. 1G). Moreover, the pan-caspase inhibitor Z-VAD-FMK significantly reversed the increases in cleaved PARP and caspase-3 levels induced by GNA (Fig. 1H, Supplementary Fig. S1C). These findings suggest that GNA induces apoptosis in CAL-27 and SCC-15 cells through caspase activation.

GNA promotes apoptosis via the upregulation of Noxa in OSCC cells

Given the association of Noxa induction with the apoptotic process, we examined the effect of GNA on Noxa expression in CAL-27 and SCC-15 cells. Western blotting analysis demonstrated that GNA significantly increased Noxa protein expression levels in a concentration- and time-dependent manner (Figs. 2A and 2B, Supplementary Figs. S1D and S1E). Additionally, GNA treatment resulted in a significant elevation of Noxa mRNA levels in both cell lines (Fig. 2C).

To further investigate the role of Noxa in GNA-induced apoptosis, we generated Noxa-knockdown cells using a shRNA system. GNA treatment induced apoptosis and increased the levels of cleaved PARP and cleaved caspase-3 in control shRNA (NC-shRNA) CAL-27 and SCC-15 cells. However, these effects were significantly attenuated in Noxa-knockdown (Noxa-shRNA) cells (Fig. 2D, Supplementary Fig. S1F). Correspondingly, the proportion of apoptotic cells was markedly reduced in the Noxa-shRNA group compared to the control group (Fig. 2E). These findings collectively indicate that Noxa is crucial for GNA-induced apoptosis in OSCC cells.

Accumulation of ROS induced by GNA is involved in OSCC cell apoptosis

ROS, as signaling molecules, play crucial roles in apoptosis in response to cellular stress. We investigated the effects of GNA on ROS production using the fluorescent probe DCFH-DA. The results indicated that GNA treatment significantly enhanced ROS production in CAL-27 and SCC-15 cells compared to untreated cells (Fig. 3A). To confirm the increase in ROS accumulation, the antioxidant NAC was used. NAC effectively blocked GNA-induced ROS accumulation in both cell lines (Fig. 3B). Furthermore, GNA exposure decreased the levels of antioxidant enzymes, including superoxide dismutases (SODs) and catalase (Fig. 3C, Supplementary Fig. S2A), suggesting that GNA induces excessive oxidative stress.

To further determine the contribution of ROS to GNA-induced cell growth inhibition and apoptosis, we examined whether NAC could antagonize GNA. CAL-27 and SCC-15 cells were pretreated with NAC to inhibit ROS. The results demonstrated that NAC completely abolished GNA-induced growth inhibition and significantly reduced the proportion of apoptotic cells (Figs. 3D and 3E). Additionally, GNA-induced increases in cleaved PARP and cleaved caspase-3 levels were blocked by NAC (Fig. 3F, Supplementary Fig. S2B). Since Noxa activation promotes mitochondrial damage, which is regulated by excessive ROS accumulation, we investigated whether GNA-induced Noxa upregulation is associated with ROS production. Our findings revealed that NAC significantly attenuated GNA-induced Noxa upregulation (Fig. 3F, Supplementary Fig. S2B). Collectively, these results indicate that ROS accumulation is essential for GNA-induced Noxa activation and apoptosis in CAL-27 and SCC-15

cells.

GNA-induced Noxa upregulation leads to apoptosis by causing ROS-mediated ER stress

Previous studies have demonstrated that ROS are linked to ER stress and cell death [10]. In our study, CAL-27 and SCC-15 cells were treated with GNA, and the levels of ER stress-related proteins were analyzed. Western blotting results showed that GNA significantly increased the expression levels of ER stress markers, including IRE1α, p-IRE1α, GRP78, ATF6, and CHOP, in a concentration- and time-dependent manner (Figs. 4A and 4B, Supplementary Figs. S2C and S2D). Furthermore, pretreatment with the antioxidant NAC inhibited the GNA-induced upregulation of ER stress-related proteins (Fig. 4C, Supplementary Fig. S2E), suggesting that GNA induces ROS-dependent ER stress. To further investigate the role of ER stress in GNA-induced cell growth

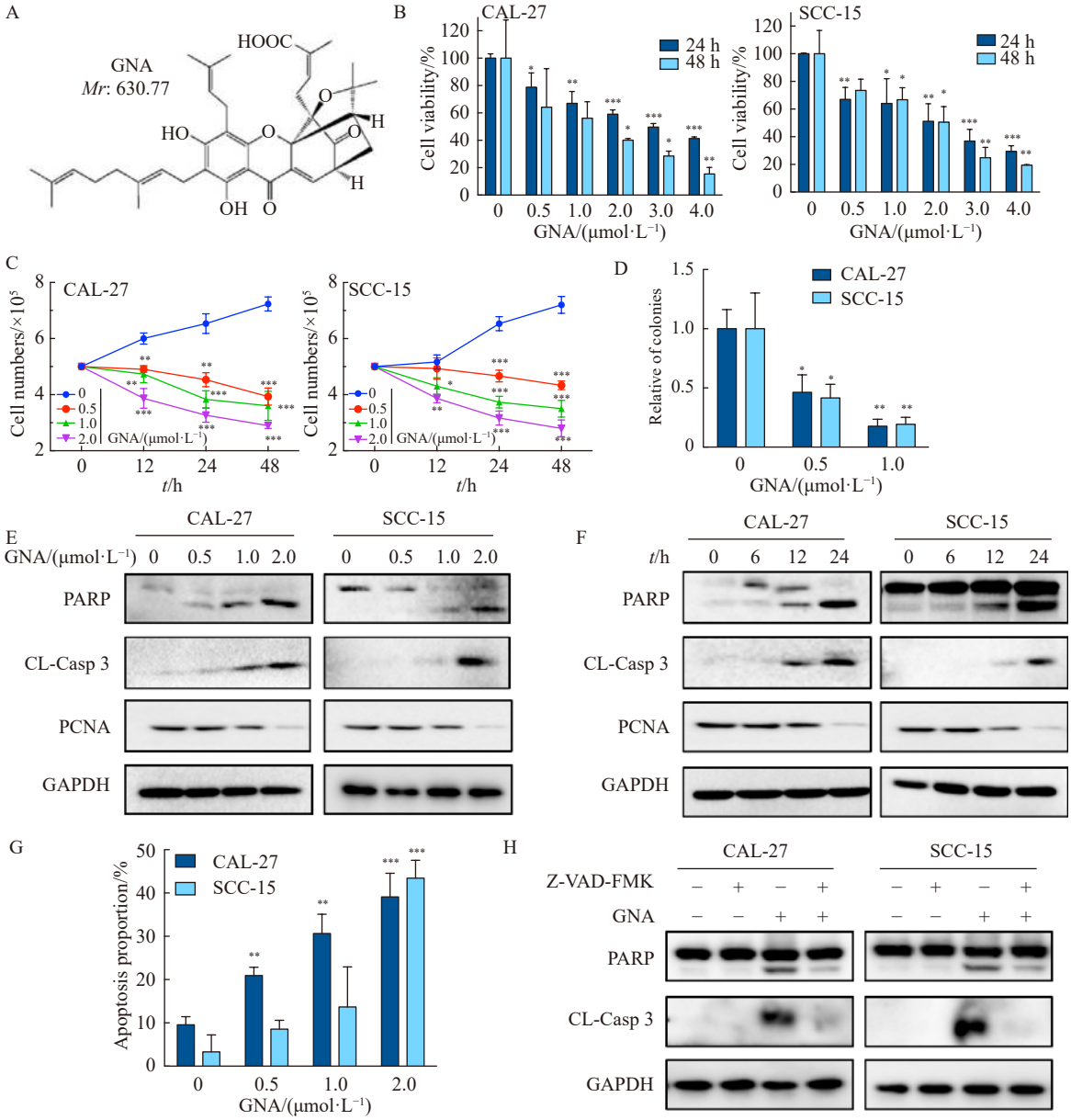

Fig. 1 GNA inhibits proliferation and induces apoptosis in human OSCC cells. (A) Chemical structure of GNA. (B) CAL-27 and SCC-15 cells were incubated with various concentrations of GNA for 24 and 48 h. OSCC cell proliferation was examined by MTT assays. (C) Trypan blue staining assays of CAL-27 and SCC-15 cells were performed. (D) Colony formation assays were performed in CAL-27 and SCC-15 cells. (E, F) CAL-27 and SCC-15 cells were treated with the indicated concentrations of GNA for 24 h (E) or GNA (2.0 μmol·L^{-1}) for 0, 6, 12, and 24 h (F). The levels of cleaved PARP, cleaved caspase-3, and PCNA were measured by Western blotting. (G) CAL-27 and SCC-15 cells were treated with GNA for 24 h, and the proportion of apoptotic cells was measured by flow cytometry. (H) CAL-27 and SCC-15 cells were incubated with or without GNA (2.0 μmol·L^{-1}) for 24 h after 2 h of pretreatment of the caspase inhibitor Z-VAD-FMK (20 μmol·L^{-1}). The levels of cleaved PARP and cleaved caspase-3 were measured by Western blotting. Data are presented as the mean ± SD (n = 3). $^{*}P$ < 0.05, $^{**}P$ < 0.01, $^{***}P$ < 0.001 *vs* control.

inhibition and apoptosis, CAL-27 and SCC-15 cells were pretreated with the ER stress inhibitor 4-PBA. Treatment with 4-PBA significantly attenuated the growth inhibition and reduced the proportion of apoptotic cells induced by GNA (Figs. 4D and 4E). Additionally, 4-PBA blocked the GNA-induced increase in cleaved PARP and cleaved caspase-3 levels (Fig. 4F, Supplementary Fig. S2F). Notably, 4-PBA also decreased the GNA-induced Noxa protein levels (Fig. 4F, Supplementary Fig. S2F). These findings indicate that GNA promotes apoptosis in OSCC cells by inducing ROS-mediated ER stress, which in turn leads to the upregulation of Noxa.

Previous studies have shown that ER stress is activated by the formation of the IRE1α-TRAF2-ASK1 complex [11]. Our results demonstrated that GNA markedly increased the expression levels of TRAF2 and phosphorylated ASK1 (p-ASK1) (Fig. 4G, Supplementary Fig. S2G). To further explore the effects of GNA on the interaction between IRE1α with TRAF2 and ASK1, we performed co-immunoprecipitation assays. As shown in Fig. 4H, The results indicated that GNA enhanced the association of IRE1α with both TRAF2 and ASK1 (Fig. 4H, Supplementary Fig. S2H). To confirm the role of ER stress in GNA-induced apoptosis, cells were transfected with IRE1α siRNA. Compared to control NC siRNA, IRE1α knockdown attenuated GNA-induced Noxa upregulation and apoptosis, as evidenced by reduced levels of cleaved PARP and cleaved caspase-3 (Fig. 4I, Supplementary Figs. S2I and S2J). Since CHOP also plays a significant role in ER stress activation [12], and GNA significantly increased the levels of ATF6 and CHOP in a concentration- and time-dependent manner (Figs. 4A and 4B), we examined the relationship between CHOP and GNA-induced Noxa upregulation and apoptosis. Notably, CHOP knockdown blocked

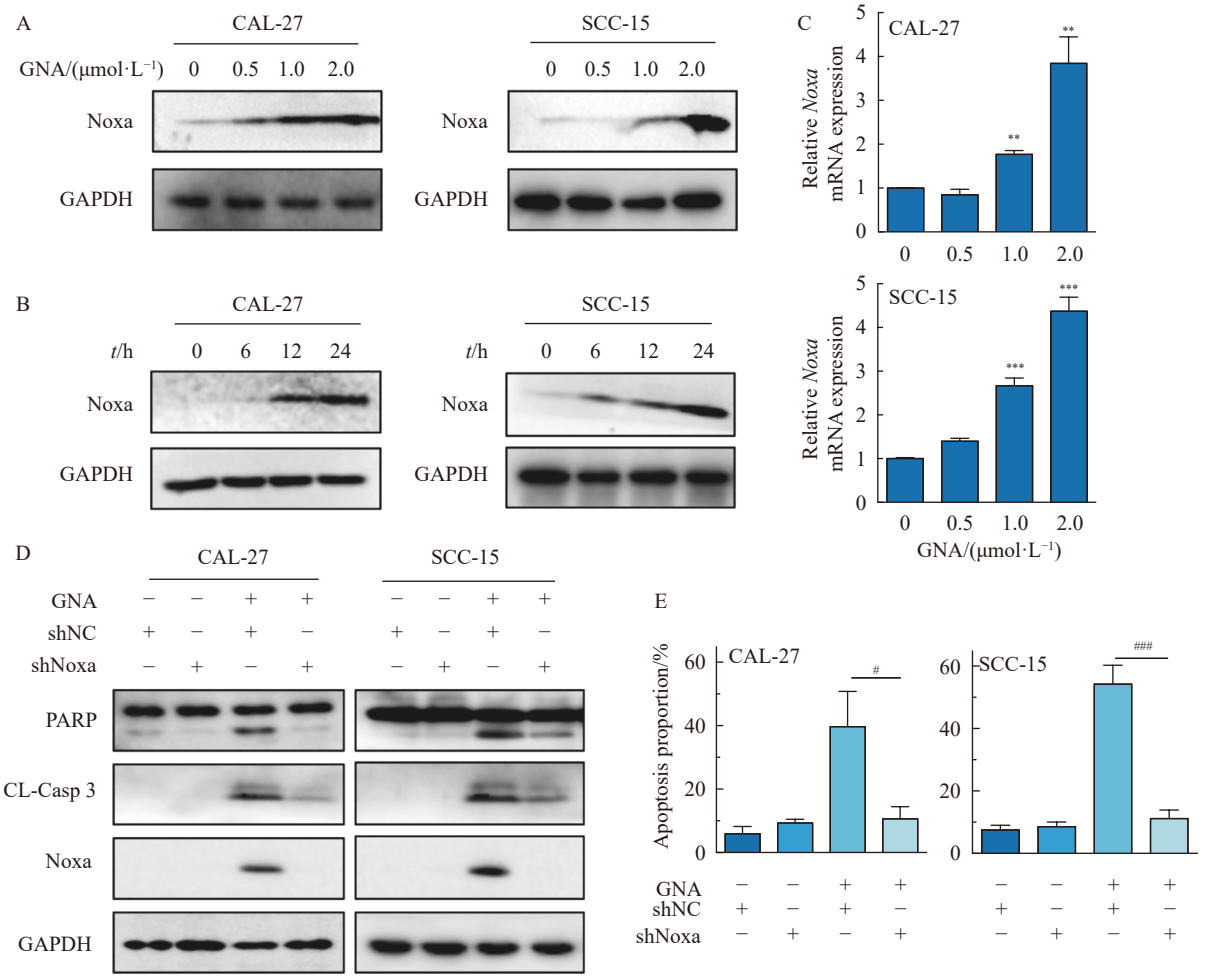

Fig. 2 GNA promotes apoptosis by upregulating Noxa in OSCC cells. (A, B) CAL-27 and SCC-15 cells were incubated with the indicated concentrations of GNA (0, 0.5, 1.0, and 2.0 μmol·L^{-1}) for 24 h or treated with 2 μmol·L^{-1} GNA for different times (0, 6, 12, and 24 h). The protein expression of Noxa was examined by Western blotting. (C) Treatment with GNA at the indicated concentrations for 24 h resulted in an increase in *Noxa* mRNA expression. (D) NC-shRNA and Noxa-shRNA cells were treated with 2 μmol·L^{-1} GNA, and the levels of cleaved PARP, cleaved caspase-3, and Noxa protein were examined by Western blotting assay. (E) The proportion of apoptotic cells was examined in NC-shRNA and Noxa-shRNA CAL-27 and SCC-15 cells after 2 μmol·L^{-1} GNA treatment. Data are presented as the mean ± SD (n = 3). $^{**}P < 0.01$, $^{***}P < 0.001$ *vs* control; $^{\#}P < 0.05$, $^{\#\#\#}P < 0.001$ *vs* GNA treatment.

GNA-induced Noxa upregulation and the increases in cleaved PARP and cleaved caspase-3 levels (Fig. 4J, Supplementary Figs. S2K and S2L). Together, these data suggest that excessive ROS and ER stress contribute to GNA-induced Noxa upregulation and apoptotic cell death. The activation of the IRE1α-TRAF2-ASK1 complex, as well as the involvement of CHOP, are critical components in this apoptotic pathway.

Activation of JNK signaling is critical for GNA-induced Noxa-dependent apoptosis in OSCC cells

The activation of the IRE1α-TRAF2-ASK1 axis is known to induce JNK activation, which plays a crucial role in regulating cell proliferation and differentiation and apoptotic cell death [13]. In our study, CAL-27 and SCC-15 cells treated with GNA at various concentrations and time points showed a significant increase in phosphorylated JNK levels (Figs. 5A and 5B, Supplementary Figs. S3A and S3B). To investigate the relationship between ER stress and GNA-induced JNK activation, we treated cells with the ER stress inhibitor 4-PBA. The results indicated that 4-PBA effectively blocked GNA-induced JNK activation (Fig. 5C, Supplementary Fig. S3C). Moreover, IRE1α knockdown significantly reversed the increases in JNK phosphorylation in CAL-27 and SCC-15 cells after GNA treatment (Fig. 5D, Supplementary Fig. S3D).

To explore the role of JNK in GNA-induced apoptosis, we examined whether blocking JNK activity could reverse GNA-induced cell growth inhibition and apoptosis. The JNK inhibitor SP600125 significantly attenuated the inhibitory effects of GNA on cell growth (Fig. 5E). Furthermore, our data demonstrated that SP600125 abrogated GNA-induced apoptosis and Noxa upregulation in CAL-27 and SCC-15 cells (Figs. 5F and 5G, Supplementary Fig. S3E). Similarly, the

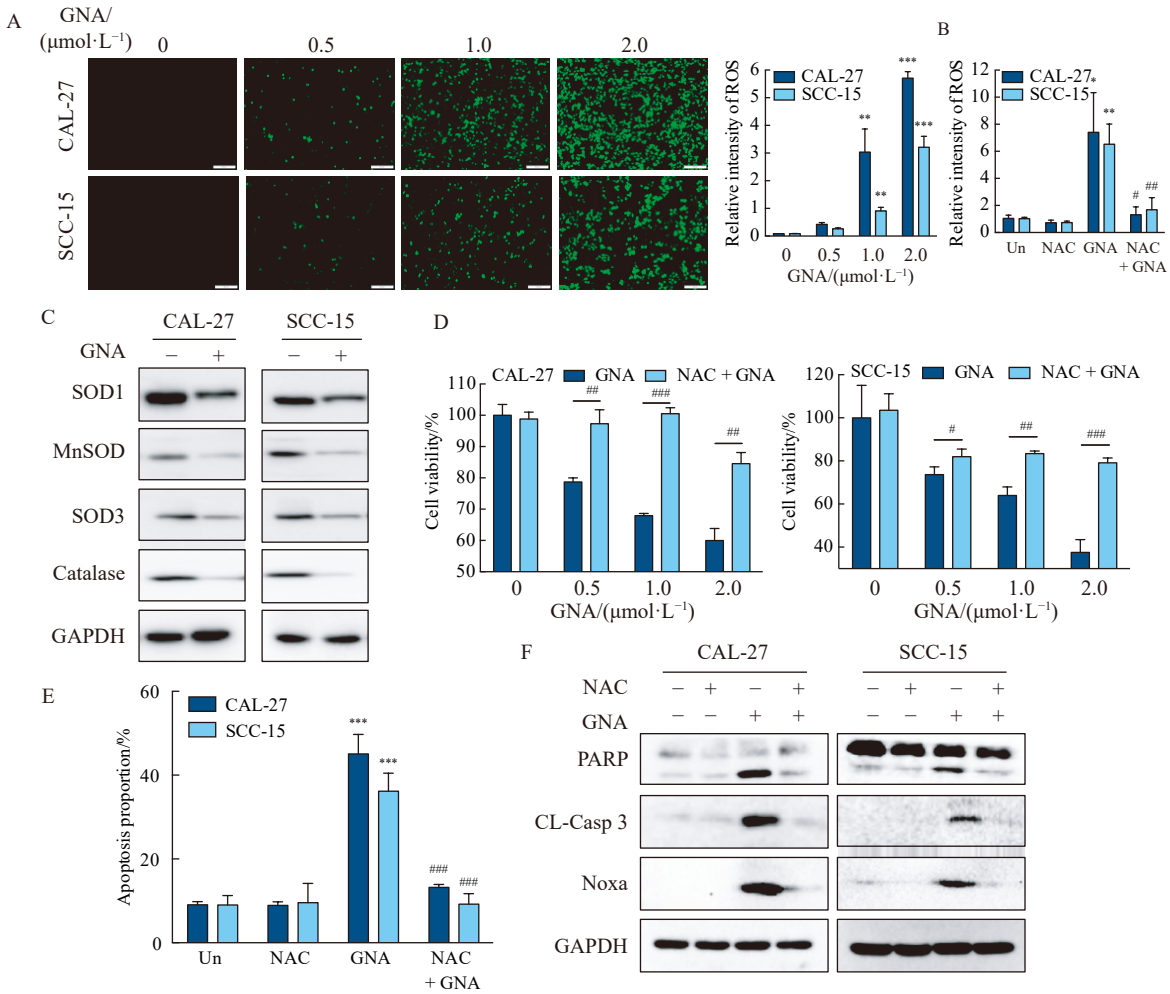

Fig. 3 The accumulation of ROS induced by GNA is involved in OSCC cell apoptosis. (A) CAL-27 and SCC-15 cells were incubated with GNA for 12 h, and the level of ROS was examined by fluorescence microscopy. (B) CAL-27 and SCC-15 cells were pre-incubated with NAC for 2 h and then cocultured with GNA for 12 h. The level of ROS was examined. (C) The antioxidant proteins were determined by Western blotting assay. (D−F) CAL-27 and SCC-15 cells were pretreated with NAC for 2 h and then co-cultured with GNA for 24 h. Cell proliferation was examined by MTT assays (D), the proportion of apoptotic cells was examined by flow cytometry (E), and the levels of cleaved PARP, cleaved caspase-3, and Noxa protein expression were examined by Western blotting assay (F). Data are presented as the mean ± SD (n = 3). $^{*}P < 0.05$, $^{**}P < 0.01$, $^{***}P < 0.001$ *vs* control. $^{\#}P < 0.05$, $^{\#\#}P < 0.01$, $^{\#\#\#}P < 0.001$ *vs* GNA treatment.

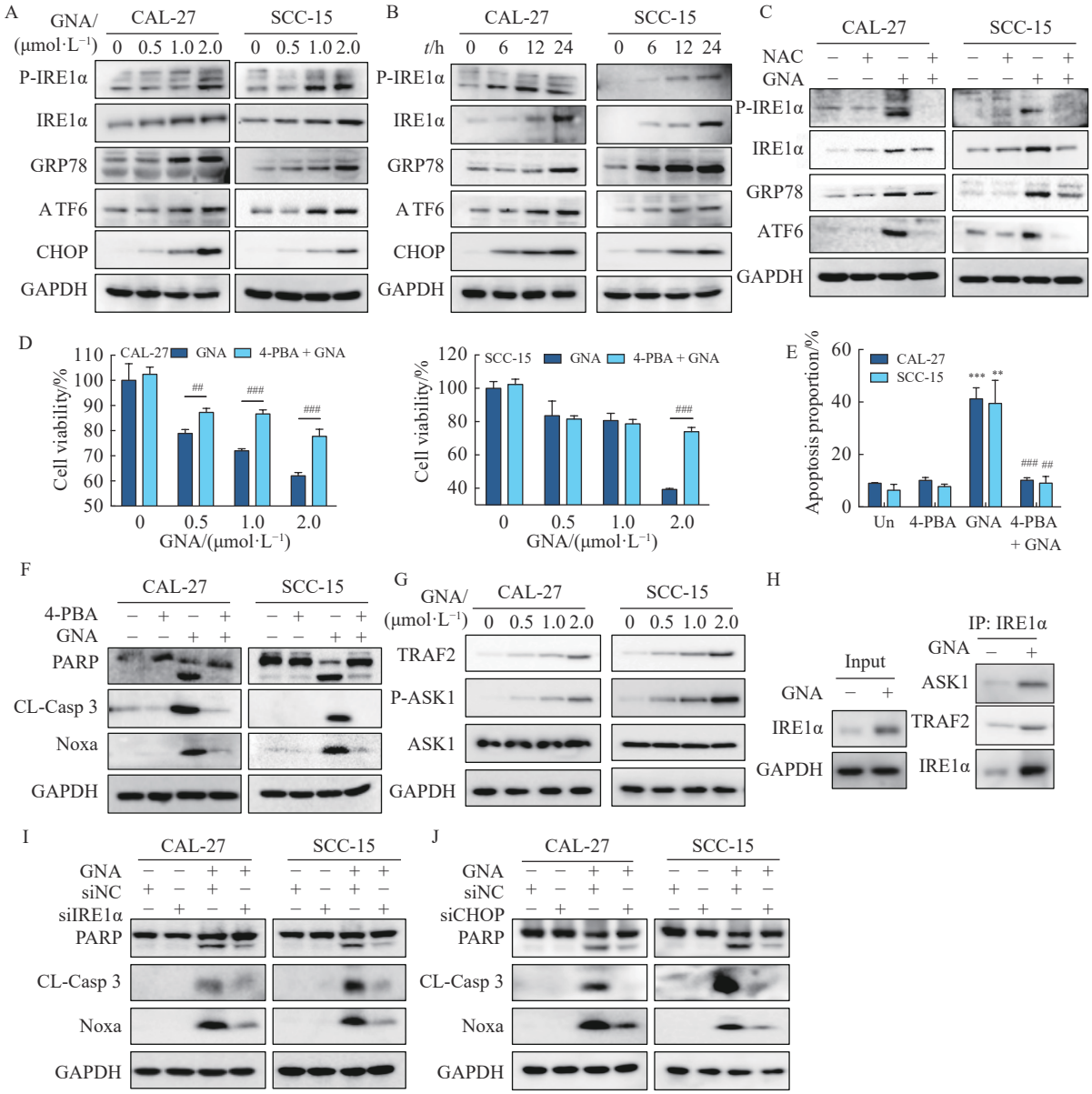

Fig. 4 GNA-induced Noxa upregulation leads to apoptosis by causing ROS-mediated ER stress. (A, B) CAL-27 and SCC-15 cells were treated with the indicated concentrations of GNA for 24 h (A) or 2.0 μmol·L^{-1} GNA for 0, 6, 12, and 24 h (B). The levels of ER stress-related proteins were examined. (C) CAL-27 and SCC-15 cells were treated with GNA for 24 h and exposed to NAC. The levels of ER stress-related proteins (GRP78, p-IRE1α, IRE1α, ATF6, and CHOP) were examined by Western blotting assay. (D−F) CAL-27 and SCC-15 cells were pretreated with 4-PBA for 2 h and then cocultured with GNA for 24 h. Cell proliferation was examined by MTT assays (D), the proportion of apoptotic cells was examined by flow cytometry (E), and the levels of cleaved PARP, cleaved caspase-3, and Noxa protein expression were examined (F). (G) CAL-27 and SCC-15 cells were treated with different concentrations of GNA for 24 h. The protein levels of TRAF2, p-ASK1, and ASK1 were detected by Western blotting analysis. (H) The IRE1α/TRAF2 and IRE1α/ASK1 complexes were precipitated by IRE1α and then detected by Western blotting analysis for TRAF2 or ASK1. (I, J) Cells were transfected with siRNA NC, siRNA IRE1α (I), or siRNA CHOP (J) and then incubated with GNA, and the levels of cleaved PARP, cleaved caspase-3, and Noxa protein were examined by Western blotting assay. Data are presented as the mean ± SD (n = 3). $^{**}P < 0.01$, $^{***}P < 0.001$ *vs* control. $^{\#\#}P < 0.01$, $^{\#\#\#}P < 0.001$ *vs* GNA treatment.

GNA-induced increase in Noxa levels was suppressed by JNK1 and JNK2 knockdown in CAL-27 cells (Fig. 5H, Supplementary Fig. S3F). These results collectively suggest that ER stress-mediated JNK activation is a critical pathway for GNA-induced Noxa upregulation and subsequent apoptosis in OSCC cells.

GNA upregulates Noxa expression and ER stress/JNK activation, leading to apoptosis in vivo

To evaluate the antitumor effect of GNA *in vivo*, we established a xenograft tumor model using CAL-27 cells. Following treatment with GNA and a positive control drug, we observed that GNA significantly inhibited tumor growth

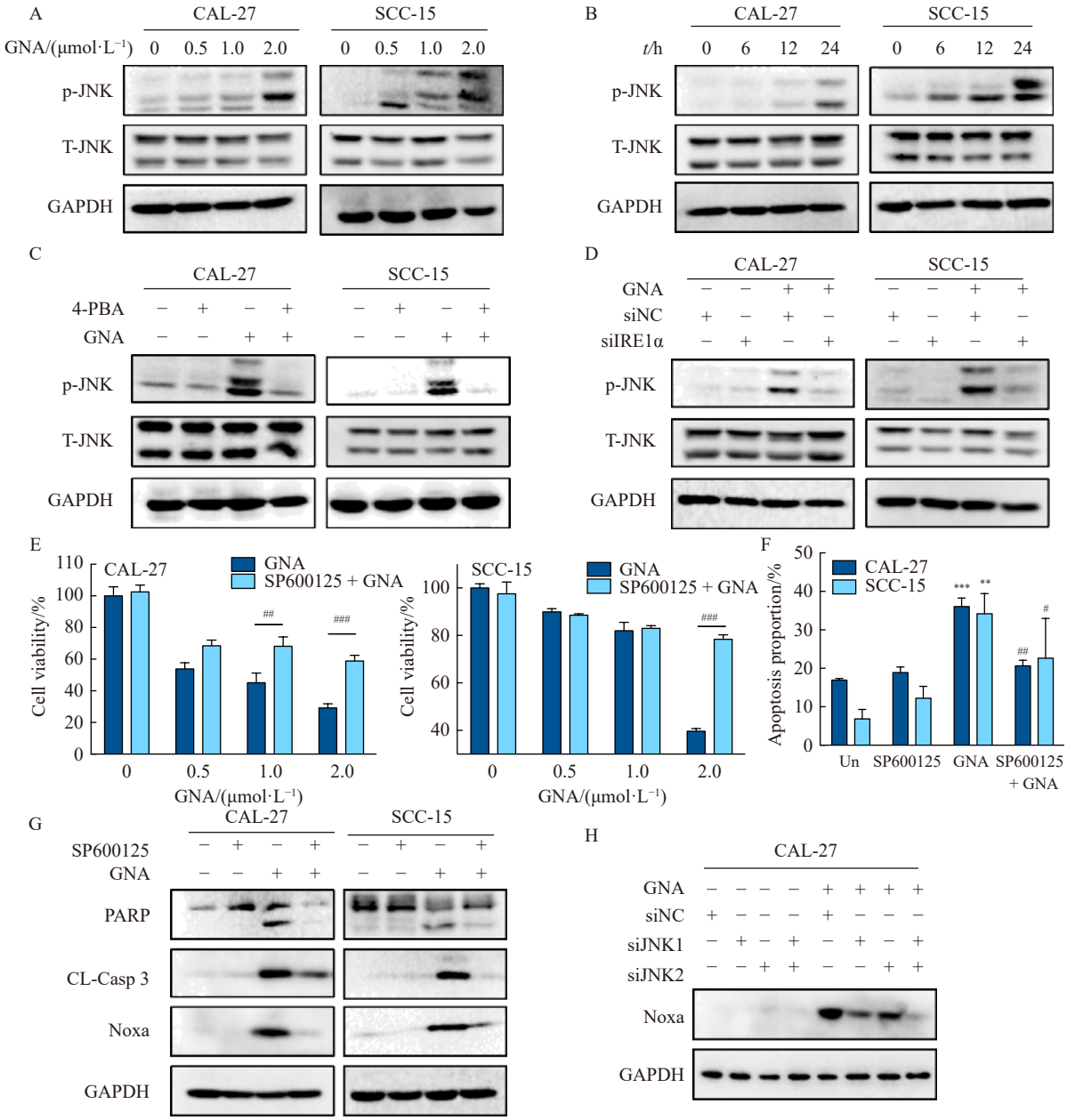

Fig. 5 JNK signaling activation is critical for GNA-induced apoptosis in OSCC cells. (A) CAL-27 and SCC-15 cells were incubated with GNA for 24 h, and the levels of p-JNK and JNK protein expression were examined by Western blotting assay. (B) Cells were treated with 2.0 μmol·L^{-1} GNA for the indicated time points. The levels of p-JNK and JNK protein expression were examined. (C) Cells were preincubated with 4-PBA and then treated with GNA for 24 h. The levels of p-JNK and JNK protein expression were examined. (D) Cells were transfected with siRNA NC or siRNA IRE1α and then incubated with GNA, and the levels of p-JNK and JNK protein expression were examined. (E−G) CAL-27 and SCC-15 cells were pretreated with SP600125 for 2 h and then incubated with GNA for 24 h. Cell proliferation was examined by MTT assays (E), and the proportion of apoptotic cells was measured by flow cytometry (F). Apoptosis was confirmed by measuring the levels of cleaved PARP, cleaved caspase-3, and Noxa protein under the same conditions (G). (H) Cells were transfected with siRNA NC, siRNA JNK1, or siRNA JNK2 and then incubated with GNA, and the levels of Noxa protein were examined by Western blotting assay. Data are presented as the mean ± SD (n = 3). $^{**}P < 0.01$, $^{***}P < 0.001$ *vs* control; $^{\#}P < 0.05$, $^{\#\#}P < 0.01$, $^{\#\#\#}P < 0.001$ *vs* GNA treatment.

without causing significant loss of body weight in the treated mice (Figs. 6A−6D). To confirm the pro-apoptotic effect of GNA *in vivo*, we conducted Western blotting analysis on xenograft tumor tissues. The results indicated that GNA treatment significantly increased the levels of cleaved caspase-3 and Noxa expression. Additionally, the levels of phosphorylated JNK (p-JNK), phosphorylated IRE1α (p-IRE1α), and total IRE1α were elevated in the xenograft tumors treated with GNA (Figs. 6E and 6F). These findings demonstrate that GNA exerts potent antitumor activity against OSCC *in vivo*, promoting apoptosis through the upregulation of Noxa and activation of the ER stress/JNK pathway while maintaining a

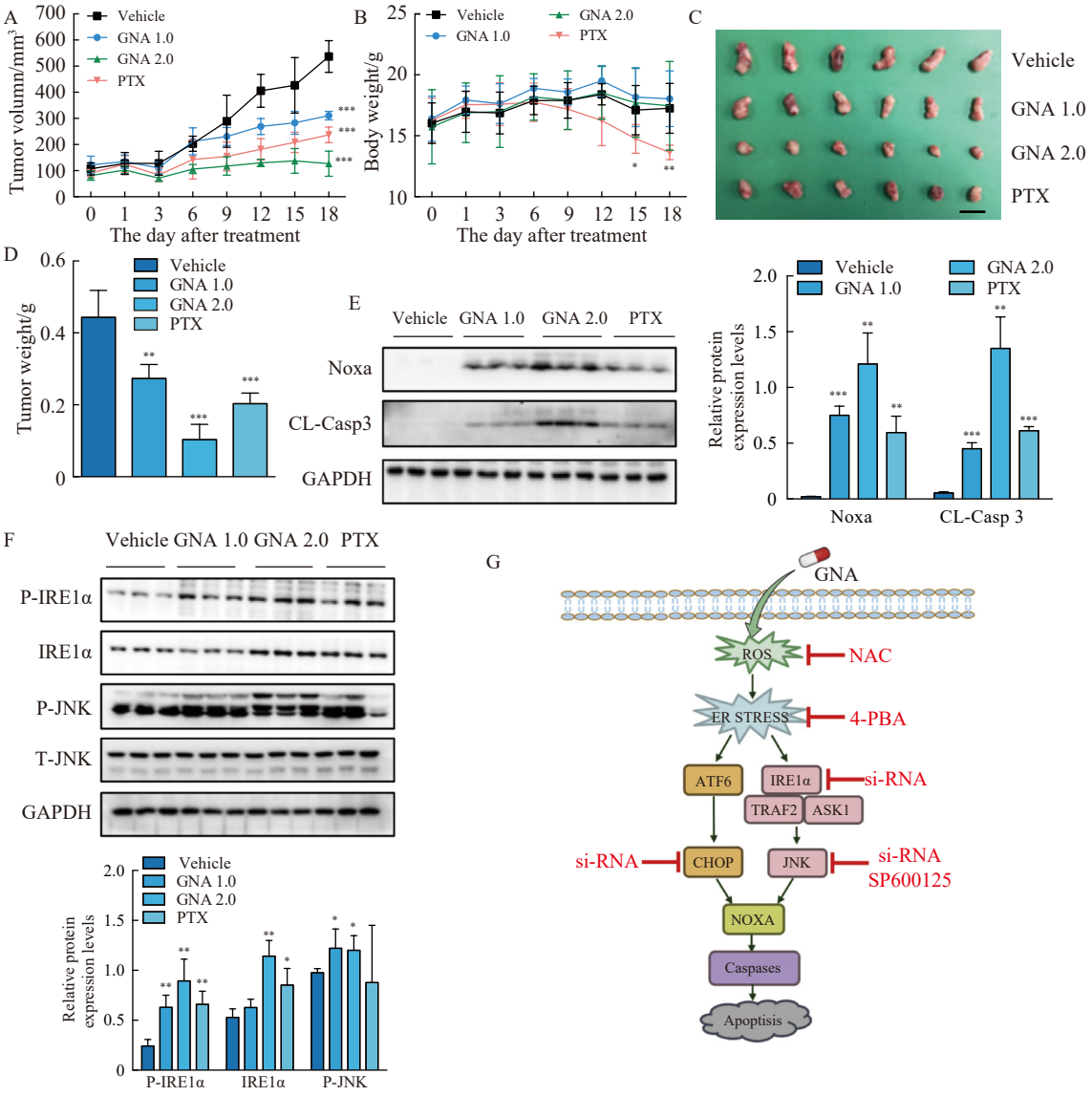

Fig. 6 GNA upregulates Noxa expression and ER stress/JNK activation, leading to apoptosis *in vivo*. (A–D) CAL-27 xenografts were established in BALB/C nude mice, and the mice were treated as indicated. Tumor volumes were measured (A), and the body weights of the mice were shown (B). Photographs of tumors were captured (C), and the weights of the tumors were recorded (D). Scale bar, 1 cm. (E, F) The levels of Noxa, cleaved caspase-3, p-IRE1α, IRE1α, p-JNK, and JNK in xenograft tumors were analyzed after drug administration. (G) The underlying mechanism of GNA's anticancer activity. Data are presented as the mean ± SD ($n = 6$ in A–D; $n = 3$ in E and F). $^{*}P < 0.05$, $^{**}P < 0.01$, $^{***}P < 0.001$ *vs* control.

high safety profile in the animal model.

Discussion

In the clinical management of OSCC, the standard treatment involves surgical resection often supplemented with chemotherapeutic drugs [14]. Therefore, there is significant interest in identifying highly effective antitumor agents with minimal toxicity for treating OSCC. GNA, a bioactive compound derived from the resin of *G. hanburyi*, has demonstrated antitumor activity across various cancer types [6, 15-17]. In this study, we investigated the antitumor effects and underlying molecular mechanisms of GNA in OSCC. Previous research has highlighted the role of apoptosis in the tumor-inhibitory effects of GNA [7, 8]. However, the specific impact of GNA on OSCC and its detailed mechanisms remain poorly understood. Here, we examined the effects of GNA on OSCC both *in vitro* and *in vivo*, focusing on the molecular pathways involved in GNA-induced apoptosis, particularly the relationship between GNA-mediated ROS/ER stress activation, Noxa upregulation, and apoptosis.

Inducing apoptosis is a crucial mechanism through which antitumor drugs exert their effects [18-22]. Our results demonstrated that GNA significantly induced apoptosis in the OSCC cell lines CAL-27 and SCC-15 in a concentration- and time-dependent manner. This was evidenced by increased levels of cleaved PARP and cleaved caspase-3, as well as a

higher proportion of Annexin V/PI double-stained cells. Additionally, GNA upregulated Noxa, a pro-apoptotic member of the Bcl-2 homology 3 domain-only protein family, in a concentration- and time-dependent manner. Notably, Noxa knockdown significantly inhibited GNA-induced apoptosis in OSCC cell lines, indicating that Noxa activation is essential for GNA-induced apoptosis. Complementary these *in vitro* findings, GNA treatment in a CAL-27 xenograft tumor model significantly suppressed tumor growth and induced apoptosis without causing adverse effects. Western blotting analysis confirmed increased levels of cleaved caspase-3 and Noxa, along with elevated levels of p-JNK, p-IRE1α, and total IRE1α in GNA-treated xenograft tumors. Collectively, these findings suggest that GNA is a potent and safe antitumor agent for OSCC. Its mechanism of action involves inducing apoptosis through Noxa upregulation, mediated by ROS/ER stress and JNK activation pathways. This study underscores the potential of GNA as an effective therapeutic strategy for OSCC, warranting further clinical investigation.

ROS are biologically significant molecules that result from the incomplete reduction of oxygen [23]. While moderate levels of ROS are essential for cell survival, proliferation, and differentiation, excessive ROS production is toxic, leading to oxidative damage and cell death [24, 25]. ROS plays a dual role in cancer, being crucial for tumor initiation and progression, as well as serving as a target for cancer therapy [26]. In this study, we observed that GNA treatment led to excessive ROS accumulation in OSCC cells. Importantly, the use of the ROS scavenger NAC effectively blocked GNA-induced cell growth inhibition and apoptosis, indicating that ROS are critical mediators of GNA-induced apoptotic cell death and Noxa upregulation.

Excessive ROS has been shown to interfere with ER stress [27]. ER stress activates the unfolded protein response (UPR), which is integral to cell apoptosis [28]. The UPR comprises three main pathways: IRE1, ATF6, and PKR-like endoplasmic reticulum kinase (PERK) [29]. Our findings demonstrated that GNA elevated levels of ER stress-related proteins in OSCC cells, which could be attenuated by NAC, suggesting that ROS accumulation precedes and regulates GNA-induced ER stress. IRE1 is a crucial regulator of ER stress, acting as a transmembrane protein that, upon activation, recruits TRAF2. TRAF2 subsequently binds to ASK1, forming the IRE1α-TRAF2-ASK1 complex and activating the JNK signaling pathway [13]. Our study showed that GNA-induced apoptosis and Noxa upregulation in OSCC cells are mediated through ER stress-induced JNK activation *via* the IRE1α-TRAF2-ASK1 complex. Additionally, the induction of ATF6 and CHOP, which are sensitive to ER stress, further supports the role of ER stress in GNA's mechanism of action [30]. CHOP knockdown attenuated GNA-induced Noxa upregulation and apoptosis, reinforcing the significance of the ATF6-CHOP pathway in this process. Collectively, these results suggest that excessive ROS/ER stress contributes to GNA-dependent Noxa upregulation and apoptotic cell death by activating the IRE1α-TRAF2-ASK1-mediated JNK signaling pathway and the ATF6-CHOP signaling pathway.

In summary, GNA induces apoptotic cell death in OSCC cells *in vitro* and *in vivo*. The induction of apoptosis by GNA is associated with ROS-mediated ER stress activation, which in turn leads to Noxa upregulation (Fig. 6G). These findings provide a strong rationale for the further development of GNA as a therapeutic agent for OSCC, highlighting its potential efficacy and safety.

Supporting Information

Supporting information of this paper can be requested by sending E-mails to the corresponding authors.

References

[1] Siegel RL, Miller KD, Fuchs HE, *et al*. Cancer statistics, 2022 [J]. *Ca-Cancer J Clin*, 2022, **72**(1): 7-33.

[2] Gröbe A, Blessmann M, Hanken H, *et al*. Prognostic relevance of circulating tumor cells in blood and disseminated tumor cells in bone marrow of patients with squamous cell carcinoma of the oral cavity [J]. *Clin Cancer Res*, 2014, **20**(2): 425-433.

[3] Wang J, Thomas HR, Li Z, *et al*. Puma, Noxa, p53, and p63 differentially mediate stress pathway induced apoptosis [J]. *Cell Death Dis*, 2021, **12**(7): 659.

[4] Delbridge ARD, Strasser A. The BCL-2 protein family, BH3-mimetics and cancer therapy [J]. *Cell Death Differ*, 2015, **22**(7): 1071-1080.

[5] Jia BY, Li SS, Hu XR, *et al*. Recent research on bioactive xanthones from natural medicine: *Garcinia hanburyi* [J]. *AAPS PharmScitech*, 2015, **16**(4): 742-758.

[6] Yu XJ, Han QB, Wen ZS, *et al*. Gambogenic acid induces G_1 arrest *via* GSK3 beta-dependent cyclin D1 degradation and triggers autophagy in lung cancer cells [J]. *Cancer Lett*, 2012, **322**(2): 185-194.

[7] Zhao Q, Zhong J, Bi Y, *et al*. Gambogenic acid induces Noxa-mediated apoptosis in colorectal cancer through ROS-dependent activation of IRE1 alpha/JNK [J]. *Phytomedicine*, 2020, **78**: 153306.

[8] Wu JJ, Wang DJ, Zhou JY, *et al*. Gambogenic acid induces apoptosis and autophagy through ROS-mediated endoplasmic reticulum stress *via* JNK pathway in prostate cancer cells [J]. *Phytother Res*, 2023, **37**(1): 310-328.

[9] Liu ZL, Wang XZ, Li JP, *et al*. Gambogenic acid induces cell death in human osteosarcoma through altering iron metabolism, disturbing the redox balance, and activating the P53 signaling pathway [J]. *Chem Biol Interact*, 2023, **382**: 110602.

[10] Jeong S, Yun HK, Jeong YA, *et al*. Cannabidiol-induced apoptosis is mediated by activation of Noxa in human colorectal cancer cells [J]. *Cancer Lett*, 2019, **447**: 12-23.

[11] Zhang RK, Wang P, Lu YC, *et al*. Cadmium induces cell centrosome amplification *via* reactive oxygen species as well as endoplasmic reticulum stress pathway [J]. *J Cell Physiol*, 2019, **234**(10): 18230-18248.

[12] Liu N, Yang HL, Wang P, *et al*. Functional proteomic analysis revels that the ethanol extract of *Annona muricata* L. induces liver cancer cell apoptosis through endoplasmic reticulum stress pathway [J]. *J Ethnopharmacol*, 2016, **189**: 210-217.

[13] Yu YM, Wu DX, Li YW, *et al*. Ketamine enhances autophagy and endoplasmic reticulum stress in rats and SV-HUC-1 cells *via* activating IRE1-TRAF2-ASK1-JNK pathway [J]. *Cell Cycle*, 2021, **20**(18): 1907-1922.

[14] Saha SK, Khuda-Bukhsh AR. Molecular approaches towards

development of purified natural products and their structurally known derivatives as efficient anti-cancer drugs: current trends [J]. *Eur J Pharmacol*, 2013, **714**(1-3): 239-248.
[15] Xu LF, Meng XX, Xu NH, *et al*. Gambogenic acid inhibits fibroblast growth factor receptor signaling pathway in erlotinib-resistant non-small-cell lung cancer and suppresses patient-derived xenograft growth [J]. *Cell Death Dis*, 2018, **9**(3): 262.
[16] Wang M, Li SS, Wang YL, *et al*. Gambogenic acid induces ferroptosis in melanoma cells undergoing epithelial-to-mesenchymal transition [J]. *Toxicol Appl Pharm*, 2020, **401**: 115110.
[17] Zhou SM, Zhao N, Wang JL. Gambogenic acid suppresses bladder cancer cells growth and metastasis by regulating NF-*κ*B signaling [J]. *Chem Biol Drug Des*, 2020, **96**(5): 1272-1279.
[18] Li XL, He SH, Liang W, *et al*. Marsdenia tenacissima injection induces the apoptosis of prostate cancer by regulating the AKT/GSK3β/STAT3 signaling axis [J]. *Chin J Nat Med*, 2023, **21**(2): 113-126.
[19] Wang GY, Zhang L, Geng YD, *et al*. *β*-Elemene induces apoptosis and autophagy in colorectal cancer cells through regulating the ROS/AMPK/mTOR pathway [J]. *Chin J Nat Med*, 2022, **20**(1): 9-21.
[20] Du BX, Lin P, Lin J. EGCG and ECG induce apoptosis and decrease autophagy the AMPK/mTOR and PI3K/AKT/mTOR pathway in human melanoma cells [J]. *Chin J Nat Med*, 2022, **20**(4): 290-300.
[21] Zhang Y, Qu Y, Chen YZ. Influence of 6-shogaol potentiated on 5-fluorouracil treatment of liver cancer by promoting apoptosis and cell cycle arrest by regulating AKT/mTOR/MRP1 signalling [J]. *Chin J Nat Med*, 2022, **20**(5): 352-363.
[22] Jiang X, Yang X, Shi Y, *et al*. Maackiain inhibits proliferation and promotes apoptosis of nasopharyngeal carcinoma cells by inhibiting the MAPK/Ras signaling pathway [J]. *Chin J Nat Med*, 2023, **21**(3): 185-196.
[23] Uttara B, Singh AV, Zamboni P, *et al*. Oxidative stress and neurodegenerative diseases: a review of upstream and downstream antioxidant therapeutic options [J]. *Curr Neuropharmacol*, 2009, **7**(1): 65-74.
[24] Chandra-Kuntal K, Lee J, Singh SV. Critical role for reactive oxygen species in apoptosis induction and cell migration inhibition by diallyl trisulfide, a cancer chemopreventive component of garli [J]. *Breast Cancer Res Treat*, 2013, **138**(1): 69-79.
[25] D'Autréaux B, Toledano MB. ROS as signalling molecules: mechanisms that generate specificity in ROS homeostasis [J]. *Nat Rev Mol Cell Bio*, 2007, **8**(10): 813-824.
[26] Wang SF, Chang YL, Tzeng YD, *et al*. Mitochondrial stress adaptation promotes resistance to aromatase inhibitor in human breast cancer cells *via* ROS/calcium up-regulated amphiregulin-estrogen receptor loop signaling [J]. *Cancer Lett*, 2021, **523**: 82-99.
[27] Malhotra JD, Kaufman RJ. Endoplasmic reticulum stress and oxidative stress: a vicious cycle or a double-edged sword [J]. *Antioxid Redox Signal*, 2007, **9**(12): 2277-2293.
[28] Sovolyova N, Healy S, Samali A, *et al*. Stressed to death-mechanisms of ER stress-induced cell death [J]. *Biol Chem*, 2014, **395**(1): 1-13.
[29] Bhat TA, Chaudhary AK, Kumar S, *et al*. Endoplasmic reticulum-mediated unfolded protein response and mitochondrial apoptosis in cancer [J]. *Biochim Biophys Acta Rev Cancer*, 2017, **1867**(1): 58-66.
[30] Ishteyaque S, Yadav KS, Verma S, *et al*. CYP2E1 triggered GRP78/ATF6/CHOP signaling axis inhibit apoptosis and promotes progression of hepatocellular carcinoma [J]. *Arch Biochem Biophys*, 2023, **745**: 109701.

Cite this article as: CHENG Xinran, FENG Mengyuan, ZHANG Anjie, *et al*. Gambogenic acid induces apoptosis *via* upregulation of Noxa in oral squamous cell carcinoma [J]. *Chin J Nat Med*, 2024, **22**(7): 632-642.